Available online at www.sciencedirect.com

ScienceDirect

Proceedings of the Combustion Institute 37 (2019) 4285–4293

Proceedings of the Combustion Institute

www.elsevier.com/locate/proci

Thermal structure of the blue whirl

Sriram Bharath Hariharan [a], Evan T. Sluder [a], Michael J. Gollner [a,*], Elaine S. Oran [b]

[a] Department of Fire Protection Engineering, University of Maryland, College Park, MD, USA
[b] Department of Aerospace Engineering, University of Maryland, College Park, MD, USA

Received 30 November 2017; accepted 16 May 2018
Available online 29 June 2018

Abstract

The blue whirl is a recently discovered regime of the fire whirl that burns without any visible soot, even while burning liquid fuels directly. This flame evolves naturally from a traditional fire whirl in a fixed-frame self-entraining fire whirl experimental setup. Here, detailed thermal measurements of the flame structure performed using thermocouples and thin-filament pyrometry are presented. Thermocouple measurements reveal a peak temperature of ∼2000 K, and 2-D temperature distributions from pyrometry measurements suggest that most of the combustion occurs in the relatively small, visibly bright, blue vortex ring. Different liquid hydrocarbon fuels such as heptane, iso-octane and cyclohexane consistently formed the blue whirl with similar thermal structures, indicating that blue whirl formation is independent of fuel type, and also that the transition from a fire whirl to a blue whirl may be influenced by vortex breakdown.

Keywords: Fire whirl; Blue whirl; Soot

1. Introduction

Fire whirls have been an important part of fire science because of the dangers they present during large urban and wildland fires [1–4]. While buoyant gases ordinarily move upward in a convection column or plume over a burning area, fire whirls result in more violent and organized convection currents resulting in a tall, slender vortex of yellow flames [2]. While investigating the formation of fire whirls over water, a new regime of the fire whirl, the "blue whirl," was recently discovered [5]. The blue whirl evolved naturally from the initial large yellow fire whirl in a fixed-frame self-entraining apparatus, without any external control of entrainment such as a rotating mesh, blowing or suction. The flame appeared as an inverted blue cone hovering directly over the water surface. Three distinct regions of this flame were identified – the lower blue cone, at the edge of which was a bright blue ring (vortex rim), and the upper purple haze region (Fig. 1).

Figure 2a shows a traditional yellow fire whirl, observed prior to blue whirl formation. This yellow color of the fire whirl originates from black body radiation of soot particles. Although the blue whirl burned directly over a small pool of fuel that floated above the water surface, it showed no visible traces of yellow, indicating nearly soot-free combustion.

* Corresponding author.
E-mail address: mgollner@umd.edu (M.J. Gollner).

https://doi.org/10.1016/j.proci.2018.05.115
1540-7489

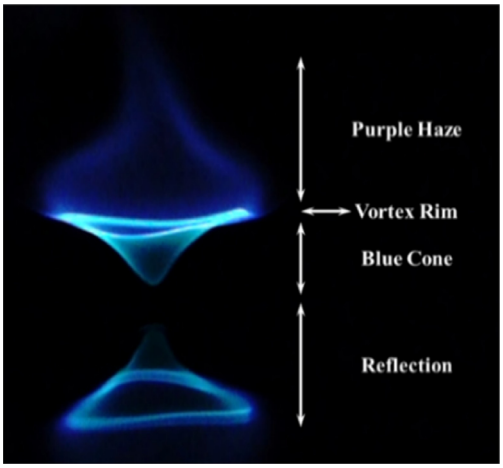

Fig. 1. Image of the blue whirl with the different regions indicated.

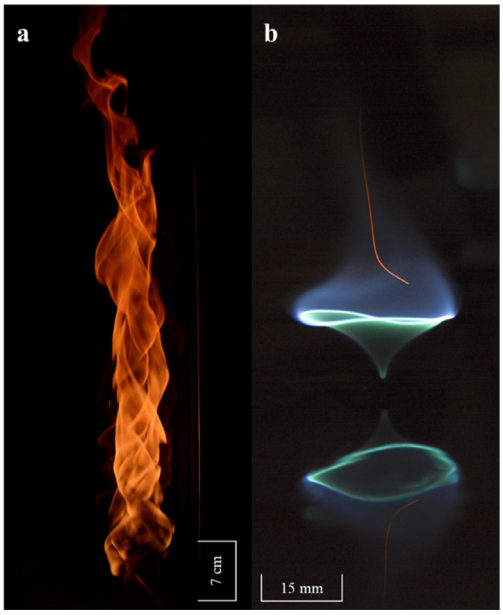

Fig. 2. Images of (a) traditional yellow fire whirl prior to blue whirl formation, and (b) a blue whirl (reflection below) showing a single soot streak.

Figure 2b (12.5 ms exposure) shows a blue whirl formed from heptane on a water surface, and shows a single yellow soot streak exiting the flame through the purple haze region.

While previous swirl combustion studies relied specifically on forced flow configurations of gaseous fuel and oxidizer to produce blue flames [6,7], the blue whirl appears over a pool of liquid fuel naturally, without any external control. As Lin and Faeth described, "soot-free hydrocarbon fueled diffusion flames are of significant interest because many practical combustion processes achieve this condition to avoid soot emissions" [8]. Thus, the blue whirl potentially offers solutions to a variety of challenges in burning liquid hydrocarbons.

2. Experimental methods

2.1. General apparatus

The fixed-frame, self-entraining fire-whirl apparatus (Figure 3) used in this study is the same as that used in a prior study in which the blue whirl was first observed [5]. The two quartz half-cylinders (32 cm dia, 60 cm high) were suspended on an aluminum frame assembled using T-slot erectors (from 80/20 Inc.). This frame allowed precise control of the position of the half-cylinders, and thus of the slit width between the two pieces. The half-cylinders were positioned such that there was no overlap, and a short overlap region (50 mm wide) was constructed along each end using aluminum tape. This allowed insertion of probes into the enclosure by removing small sections of the tape overlap at required locations. This arrangement was placed over a water pan 40 cm in diameter.

Liquid fuels used in this study were temporarily stored in a syringe (Becton Dickinson 60 ml with a Luer-Lok^{TM} Tip), and injected beneath the water surface in the pan through a copper tube (3 mm OD, 1.5 mm ID) using a syringe pump (Harvard Apparatus Pump 11 Elite). A small piece of copper wire was projected out of the opening in the copper tube. The copper wire was just below the water surface to prevent the fuel from bubbling to the surface. The syringe diameter and fuel pumping rate were programmed into the syringe pump system. The fuel used for this study is primarily 99.4% pure n-heptane, although measurements were also made with iso-octane and cyclohexane.

A typical experiment involved injection of fuel (~2.5 ml) onto the water surface, followed by ignition using a butane torch. Buoyant forces within the enclosure lead to natural self-entrainment through the slits on either side, resulting in swirling motion inside the enclosure. This initially resulted in a large yellow fire whirl, which then shrank naturally to the small, conical blue whirl. Fuel was supplied at a constant rate to maintain the flame for as long as needed for measurements to be made. Experiments were repeated with two different pan depths, 3.2 cm (stainless steel pan) and 12.2 cm (quartz pan). No discernible difference was observed in either the development of the fire whirl or the blue whirl when the pans were interchanged.

The slit width between the quartz half-cylinders determines the entrainment velocity and the swirl within the enclosure. A traditional yellow fire whirl formed over a wide range of slit widths. In this con-

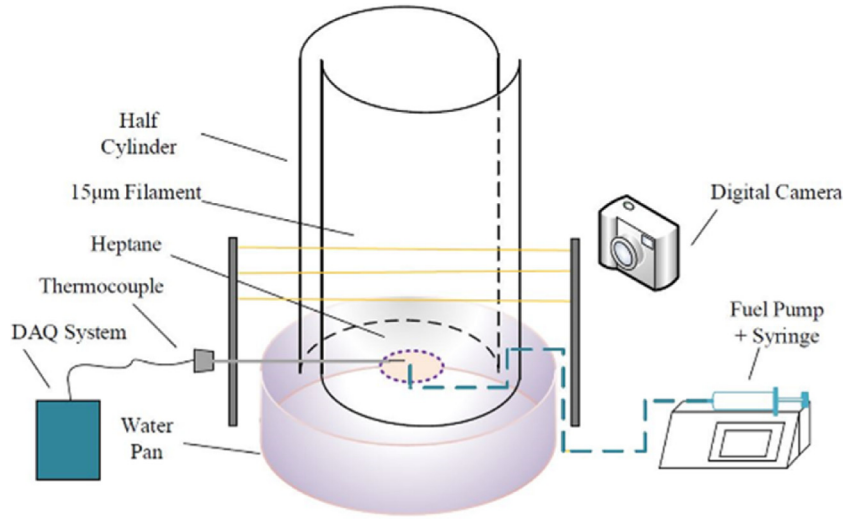

Fig. 3. Experimental apparatus.

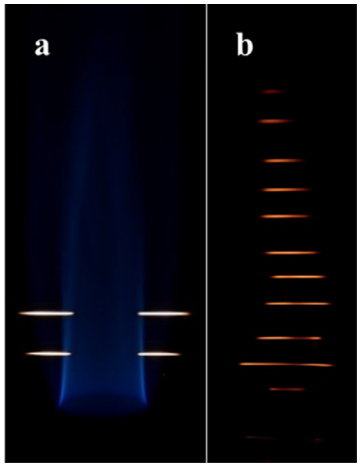

Fig. 4. (a) Image showing filaments positioned across the Bunsen burner calibration flame, (b) image of glowing filament array above a blue whirl.

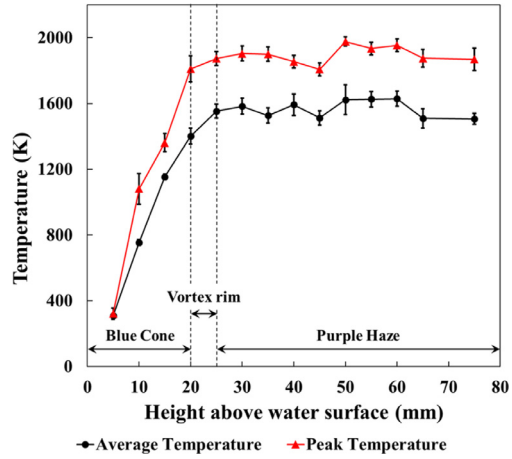

Fig. 5. Axial temperature distribution of the blue whirl formed using heptane over water, from R-type thermocouple measurements.

figuration, for a particular fuel flow rate, a relatively narrow range of slit widths led to transition from a yellow fire whirl to a blue whirl. The direction of the vortex formed inside the enclosure is determined by the orientation of the slits. In this study, both clockwise and anticlockwise orientations produced similar results, indicating Coriolis effects were negligible.

2.2. *Micro-thermocouple measurements*

A single micro-thermocouple probe was used to measure the temperature of the blue whirl. Due to continuous movement of the blue whirl in the enclosure, a steady interaction of the flame with the thermocouple bead was not possible. Since the blue whirl interacted with the thermocouple bead intermittently, these measurements were used to obtain a one-dimensional temperature distribution of the flame by adjusting the position of the thermocouple bead in the axial direction.

An R-type thermocouple (Pt/13%Rh-Pt, 50 μm) was threaded into a two-hole ceramic tube (1.6 mm OD), with the bead projecting about 5 mm out of the ceramic tube. This probe (25 cm long) was projected into the enclosure through a small slit in the aluminum tape, such that the bead was in the center of the enclosure, directly above the

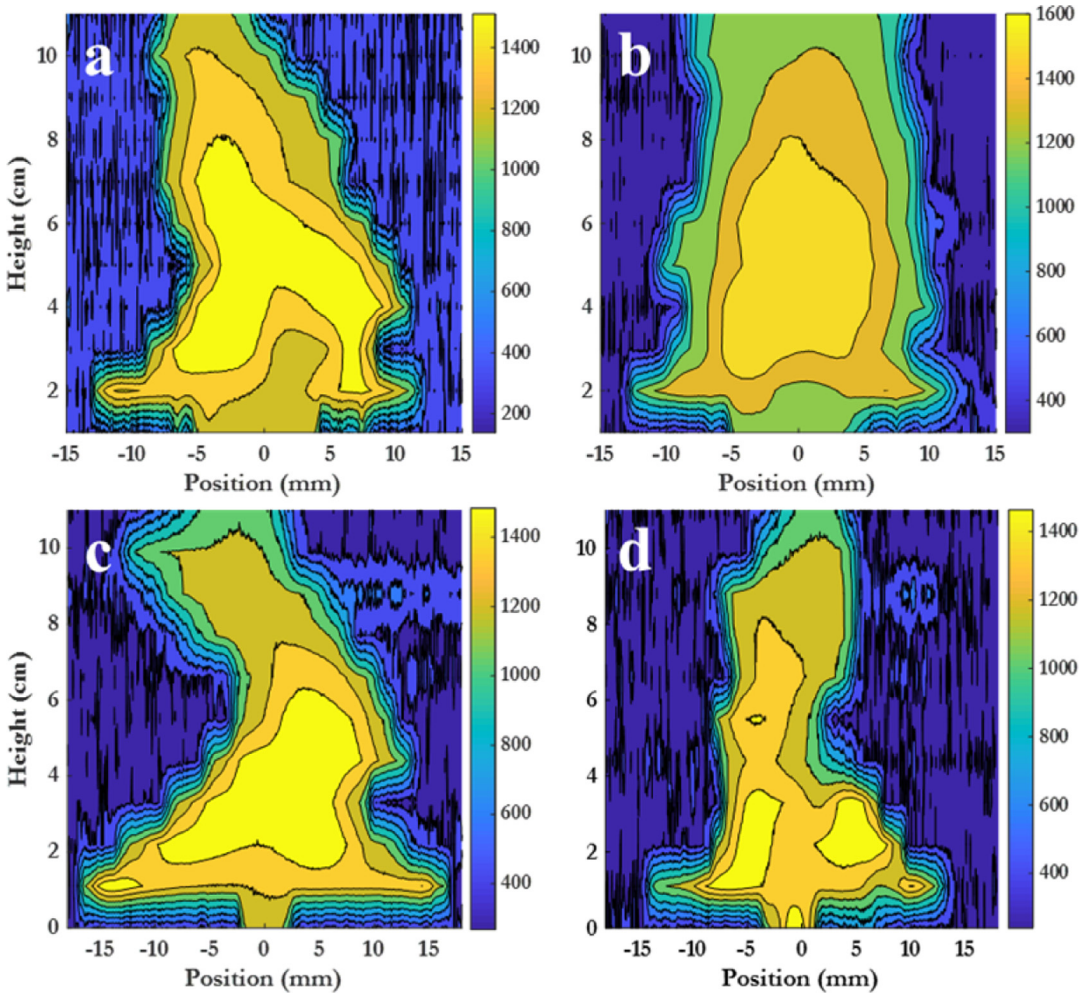

Fig. 6. (a) Instantaneous temperature of the blue whirl formed using n-heptane, (b) Average temperature map obtained from 5 images. Instantaneous temperature maps for blue whirls formed using (c) iso-octane, and (d) cyclohexane.

copper tube injecting fuel. The probe was held in place by a motor-driven traverse mechanism, which was also used to change the axial (vertical) position of the probe. Measurements were made at intervals of 5 mm, starting 5 mm above the water surface. These measurements provide radially averaged temperatures at each of these axial locations of the thermocouple bead.

The 50 μm wire diameter thermocouple had a response time of 0.02 s, and an accuracy of ±5 K [9]. Data was recorded using a NI data-acquisition system (cDAQ-9171 bus with NI TB-9214 terminal block) at 100 Hz. The continuous movement of the whirl within the enclosure caused intermittent interactions of the blue whirl with the thermocouple bead. The formation and movement of the blue whirl during the experiment was recorded using a Casio EX-F1 at 300 fps. The camera was focused on the region around the thermocouple bead, and data from the camera was used to determine the time periods when the thermocouple bead was in direct contact with the flame.

Before lighting the fuel pool for each test, the flame from the butane torch was momentarily placed over the thermocouple bead to record a spike in the temperature data log. This spike served as a marker to synchronize time stamps of the video with that of the raw thermocouple data log. Experiments were generally repeated three to five times at each axial location, depending on the number of interactions of the blue whirl with the thermocouple bead. Data from experiments where the blue whirl was steadily sustained for over three minutes were used for analysis, which ensured a sufficient number of interactions of the blue whirl with the bead. Temperatures for a maximum height of

75 mm above the water surface are reported here. Above this height, the continuous contortion and movement of the flame made it challenging to determine whether the thermocouple bead was interacting with the blue whirl.

In order to improve the accuracy of measurements, a 75 μm thermocouple was also used to obtain temperature measurements at the same vertical locations to apply a radiation correction [10]. A system of two equations (Eq. (1), one for each thermocouple, *i*) with two unknowns, T_g (gas temperature) and U (flow velocity) represents the thermal balance for each thermocouple, where T_{tc}, T_{surr}, ε_{tc}, d_w, σ are the temperature obtained from the thermocouple, ambient temperature, emissivity of the bead, bead diameter, and the Stefan–Boltzmann constant. Usually an iterative procedure is required to solve these as kinematic viscosity (ν) and thermal conductivity (k) are temperature dependent. For a first estimation however, kinematic viscosity and thermal conductivity were assumed constant. Using this procedure, the maximum radiation correction applied to the thermocouple measurements was 109 K.

$$T_g - T_{tci} = \frac{\varepsilon_{tci}\, d_{wi}\, \sigma}{k\left[0.24 + 0.56\left(\frac{U d_{wi}}{\nu}\right)^{0.45}\right]}\left(T_{tci}^4 - T_{surr}^4\right) \quad (1)$$

2.3. Thin-filament pyrometry

Thin-filament pyrometry (TFP) was used to obtain a 2-D (radial and axial) temperature distribution. Past studies have used this technique in many different combustion systems [11–16]. The procedure involves stringing SiC filaments (usually 15 μm in diameter) across a flame, causing the filaments to glow at elevated temperatures. Images of the glowing filaments are then captured by a camera and post-processed to find the luminosity of the filament in a small area of a few pixels. The relation between luminosity of the filaments and temperature is determined by thermocouple measurements of a calibration flame. Using this calibration, the filaments can then be used in other configurations to relate filament luminosity to local temperatures. An approach similar to Maun et al., [17,18] using a digital camera is followed here. The technique implemented here differs slightly in the camera used, number of filaments, properties of SiC filament material, and the calibration flame. A calibration was performed using images of two filaments positioned above a Bunsen burner (Fig. 4a). The temperature profile of the Bunsen burner was obtained using 75 μm and 125 μm R-type thermocouples. To ensure accurate calibration, the quartz half-cylinder was positioned between the burner and camera.

HI-NICALON ™ filaments (manufactured by Nippon Carbon Co., Ltd. (NCK), and supplied by COI Ceramics, Inc.) were used due to their low oxygen content (Si:C:O in the ratio 62:37:0.5) and high thermal stability, which allowed longer test periods. Filaments (600 mm in length) were stretched across the enclosure such that they passed through the small gap in-between the two quartz half-cylinders (overlap region removed for first 10 cm), to form a 2D filament array, and suspended on either side by means of tape. A total of 11 filaments were used – one every 10 mm up to a height of 10 cm above the water surface, and one at 5 mm above the water surface. Once in place, the filaments were heated before each experiment using a propane torch. This surface treatment is recommended to remove any surface coating or soot deposited on the filaments [17,18]. Figure 4b shows all the 11 filaments glowing under the influence of a blue whirl.

A Nikon D7100 camera body with an aspherical lens (DX AF-S Nikkor 18–105 mm 1:3.5-5.6 G ED) was used to capture images of the filament array. The camera was operated in full manual mode at *f*/5.6, ISO 500 and 1/1600 s shutter speed, providing a temporal resolution of 0.625 ms and a depth of field of about 6.5 mm. C_H mode (6 fps) was used to continuously capture images when the blue whirl interacted with the filament array. The focal length was 30-32 mm, giving a spatial resolution of 29 μm/pixel.

All images were recorded in NEF RAW format (large size, 6000 × 4000 pixels) in Adobe Colorspace, and converted to TIFF using Nikon ViewNX-i without any compression. The image was imported into Spotlight-16 [19] where the line profile tool was used to obtain 12-bit grayscale luminosity values across the filaments. A line width of 8 pixels perpendicular to the glowing filament was used to account for the apparent increase in luminosity compared to the non-luminous widths of the filaments. Filament luminosity was averaged over 5 pixels (parallel to glowing filament) every 0.2 mm to obtain the pertinent weighted grayscale value at the particular locations. These were then matched with the radiation-corrected thermocouple measurements of the Bunsen burner flame at the corresponding locations. The maximum radiation correction was less than 200 K.

The resulting graph of temperature as a function of grayscale luminosity followed a two-term exponential behavior, with an R^2 value of 0.95, a trend similar to that obtained by Maun et al., [18]. The calibration curve is valid up to a maximum pixel intensity of 4095, which translates to a temperature of 2105 K. The fit function (radiation-corrected temperature, T as a function of luminosity, l) is a two term exponential of the form $T(l) = ae^{bl} + ce^{dl}$, with coefficient values as follows (values indicate 95% CI): a = 1127 (971.8, 1282), b = 1.526e−4 (9.8e-5, 2.069e−4), c = −1020 (−1260, −780.1), and d = −1.537e−2 (−2.2252e−2, −8.218e−3). This calibration curve has a maximum estimated uncertainty of 80 K.

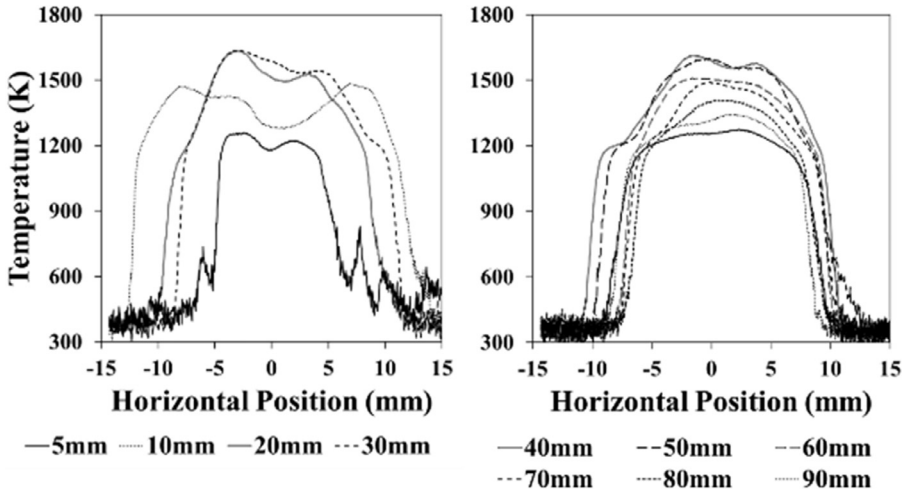

Fig. 7. Variation of average temperature with radius at selected heights above the water surface.

Background luminosity levels were very close to zero, and pixel saturation occurs beyond 2105 K. The temperature resolution of the system is 0.226 K per unit grayscale intensity, similar in behavior to [18]. Small differences are attributed to the different filament material, burner, and camera used to perform the calibration.

3. Results

3.1. Formation of the blue whirl

Upon ignition of the fuel inside the enclosure, a pool fire formed with flames around 10 cm high. After a few seconds, a yellow fire whirl began to develop, which then elongated to around 70 cm. The fuel pool spread out over the water surface upon ignition, but subsequently reduced in diameter as the fuel was consumed by the fire whirl. Typical fire whirl behavior, such as tilting [20,21] occurred, but generally for short durations.

The height of the fire whirl then continuously decreased, forming a conical fire whirl, and then finally a blue whirl. The conical and blue whirls continuously moved inside the enclosure over the water surface. The complete transition to the blue whirl typically took around 1 minute, depending on the amount of fuel initially injected onto the water surface. The height of the blue cone was around 2 cm. The size of the whirl changed continuously; when the fuel supply was stopped, the flame retained its shape (as shown in Fig. 1), but continuously diminished in size until extinction. Occasional destabilizations of the blue whirl caused a momentary transition to a small luminous fire whirl, which then spontaneously turned into a blue whirl again. A sequence of images showing this destabilization and transition back to a blue whirl has been reported in Fig. 4 of [5].

In this fixed-frame self-entraining apparatus, the gap size and fuel flow rate are the two parameters that can be controlled, and the combination of these parameters influences the shape of the fire whirl formed within the enclosure. In brief, for a gap size in the range of (15 to 55) mm, the overall range of fuel (n-heptane) flow-rate resulting in blue whirl formation was between (0.5 to 1.3) ml/min.

3.2. Axial temperature distribution

Thermocouple temperature data recorded by the DAQ was extracted based on the time stamps provided by the high speed video. At each height, approximately 1700 data points were averaged, and a radiation-corrected temperature was obtained using the procedure outlined in [10]. Figure 5 shows the resulting axial temperature distribution, with error bars indicating a 95% confidence interval. The peak temperature is obtained by averaging the highest 5% of the temperature measurements.

The data show that the temperature increases with height in the blue cone, with peak temperatures lower than 1500 K. Temperatures of the purple haze are generally higher, peaking around 2000 K. The axial location of the vortex ring is estimated to be between 20 and 25 mm above the water surface, due to the continuously changing position and size of the blue whirl.

3.3. 2-D temperature contours

If the blue whirl is assumed to be radially self-similar, thin-filament pyrometry should provide a 2-D temperature distribution in one radial plane. It is not, however, self-similar, and different regions of the blue whirl interact with the filament array

Fig. 8. Moment of transition, revealing recirculating soot patterns (40 ms exposure).

at a given instant. Due to the larger width and relatively smaller movement of the blue cone compared to the purple haze, the lower filaments had wider glowing sections (Fig. 4b).

The instantaneous temperature map derived from Fig. 4b is shown in Fig. 6a. The general structure of the contour map is similar to the visually observed features of the glowing filaments. This 2-D distribution is consistent with information obtained from the axial temperature distribution, that is, the temperature inside the blue cone increases with axial position, with the hottest region within the purple haze. The filament at 1 cm shows high temperatures at the ends, which may correspond to an interaction with the vortex rim, though the axial resolution (determined by filament spacing) is not sufficient to verify the exact location of the vortex rim using only the temperature map.

An average-temperature map (Fig. 6b) was obtained from 5 different images of the filament array over whirls formed using n-heptane. Care was taken to select images that were aligned along the same point, although the whirl was still tilting and moving. Similar alignment along the center of a fire whirl core was performed by Hartl and Smits for PIV data [22] to ensure more accurate velocity measurements, and also by Emmons and Ying for temperature data [3]. The blue cone is lower than 1400 K, and the purple haze is the hottest (Fig. 6b).

To investigate the effects of different fuels on the formation of the blue whirl and its thermal structure, thin-filament pyrometry was carried out using iso-octane and cyclohexane as the fuel. The enclosure slit widths were maintained constant, and fuel supply rates were adjusted (0.95 and 0.7 ml/min for iso-octane and cyclohexane respectively) to account for the lower rate of burning of these fuels. The instantaneous temperature contours obtained are shown in Fig. 6c,d. The temperature contours in Fig. 6 show similar thermal structures for all three fuels, with the region of the flame above the vortex rim hotter than the region below it.

4. Discussion

The blue whirl evolves from a traditional yellow fire whirl, although its physical appearance is quite different from that of the fire whirl (Fig. 2). The size is much smaller than the fire whirl, but has a higher temperature, based on previous fire whirl temperature data [23]. The blue cone region is generally lower than 1500 K. While the fire whirl burns mostly as a diffusion flame [3], the peak temperatures of 2000 K in the purple haze of the blue whirl (from thermocouple data) are around 200 K higher than expected for a non-premixed n-heptane flame [24]. These peak flame temperatures suggest the blue whirl is closer to a premixed flame, although it is unlikely that this exists throughout its flame structure.

The 2-D temperature distribution of the blue whirl (from TFP data) provides an axial and radial temperature profile. This distribution shows that the purple haze region is at a higher temperature than the blue cone region, suggesting that a large fraction of the combustion might occur just below the purple haze, in the intensely blue vortex rim region of the flame. Above 6 cm, the temperature begins to decrease, indicating that there is no further heat release in a plume of hot, reacted material. The 2-D temperature distribution for heptane (Fig. 6a,b) are in agreement with the axial distribution of average temperature obtained using microthermocouples (Fig. 5). In addition, the 2-D temperature profiles are qualitatively similar for blue whirls formed using the different fuels used in this study. The differences in the instantaneous temperature distributions (Fig. 6) are attributed to varied levels of interaction of the blue whirl with the filament array.

The spatial resolution (in the axial direction) of both of these techniques did not permit measurement of the exact temperature within the vortex rim. The maximum temperatures reported here are an estimate of the peak values due to the constant movement of the blue whirl, which causes some errors in measurement. Nonintrusive diagnostics such as quantitative schlieren [25] or thermographic PIV [26,27] may be implemented in the future to obtain more accurate values.

The average temperature obtained through TFP (Fig. 6b) from each filament is shown as a function of radius in Fig. 7. The hump-like radial distribution of temperature within the blue cone (up to ~20 mm above the water surface) is similar to results obtained for a traditional fire whirl in [3]. The hump-like temperature profile was used to determine the vortex-core edge in the fire whirl.

Following this analogy, the blue cone may form the edge of the vortex-core with maximum tangential velocities at the flame sheet.

The flame was partially destabilized by the insertion of a thermocouple probe, especially when the probe interacted with the blue cone. The destabilization caused the flame to transition into a small luminous laminar fire whirl. The same level of disturbance was not seen when the probe interacted with the purple haze region above the blue cone. Previously, the shape of the flame and its transition from the traditional fire whirl was attributed to bubble-type vortex breakdown [5]. Sensitivity to inlet flow conditions has been reported even in non-reacting bubble modes [28]. The flow field around the blue whirl is also extremely sensitive to the entrainment flow along the base, which explains the destabilization due to the probe. In attempting to visualize the change in the flame shape during a transition from a fire whirl to a blue whirl, several interesting images such as Fig. 8 were captured. Glowing streaks of remnant soot from the fire whirl help visualize the presence of recirculation zones. The recirculating pattern is similar to previous studies of non-reacting bubble-type vortex breakdown [29,30], and helps us to draw analogies to the shape of the blue whirl flame [31]. Additional study is required to understand the transition process and the role of vortex breakdown in stabilizing the flame through a combination of experimental and numerical techniques.

5. Conclusion

The thermal structure of the blue whirl was investigated using micro-thermocouples and thin-filament pyrometry. These diagnostics revealed that the flame burns hotter than expected for a diffusion flame. The thermal structure is generally independent of the specific liquid hydrocarbon fuel used in this study. It is thought that most of the energy release occurs in the bright vortex rim, leading to the high temperatures observed in the purple haze.

Use of the blue whirl in engineering applications will not be evident until the processes governing its formation are understood better, but the blue whirl regime is attractive for possible applications due to its low soot content, and formation without external mechanical forcing. While this work has shed light on the thermal structure, interesting questions remain, such as exact combinations of circulation strength and heat release leading to blue whirl formation, why the flame naturally stabilizes in the blue whirl regime, the role played by vortex breakdown and the flow field within the flame, whether the regime can be observed with gaseous fuels, and if it scales in size. These questions provide a basis to plan future experiments, and the results of this study may also be used to evaluate future numerical efforts.

Acknowledgments

The authors would like to thank Lin Jiang, Erin Griffith, Huahua Xiao, Ali Tohidi, Yu Hu, and Ajay Singh for their assistance with experiments and data analysis. This work was supported by NSF awards CBET 1507623 and 1554026, and by the University of Maryland through Minta Martin Endowment Funds (Department of Aerospace Engineering) and Glenn L. Martin Institute Chaired Professorship (A. James Clark School of Engineering).

References

[1] G.E. Byram, R.E. Martin, *Fire Control Notes* 23 (1962) 13–17.
[2] G.M. Byram, R.E. Martin, *For. Sci* 16 (1970) 386–399.
[3] H.W. Emmons, S.-J. Ying, *Proc. Combust. Inst* 11 (1967) 475–488.
[4] A. Tohidi, M.J. Gollner, H. Xiao, *Ann. Rev. Fluid Mech* (2018) 50.
[5] H. Xiao, M.J. Gollner, E.S. Oran, *Proc. Natl. Acad. Sci* 113 (2016) 9457–9462.
[6] N. Syred, J.M. Beér, *Combust. Flame* 23 (1974) 143–201.
[7] R.A. Yetter, I. Glassman, H.C. Gabler, *Proc. Combust. Inst* 28 (2000) 1265–1272.
[8] K.-C. Lin, G.M. Faeth, *Int. J. Environ. Combust. Tech* I (2000) 53–79.
[9] Omega, Thermocouple Toler. Values, Available <http://www.omega.com/techref/colorcodes.html>(n.d.) 1–7.
[10] A.V. Singh, M.J. Gollner, *Combust. Flame* 162 (2015) 2214–2230.
[11] V. Vilimpoc, L.P. Goss, B. Sarka, 13 (1988) 93–95.
[12] V. Vilimpoc, L.P. Goss, *Proc. Combust. Inst* 22 (1989) 1907–1914.
[13] S. Pauzin, A. Giovannini, B. Bédat, *Exp. Fluids* 17 (1994) 397–404.
[14] W.M. Pitts, *Symp. Combust* 26 (1996) 1171–1179.
[15] G. Wang, C. Bonilla, D. Kalitan, in: ASME Turbo Expo Turbine Technical Conference & Exposition GT2014, Dusseldorf, Germany, 2014, pp. 1–11.
[16] H. Guo, J.A. Castillo, P.B. Sunderland, *Appl. Opt* 52 (2013) 8040–8047.
[17] J.D. Maun, *Thin Filament Pyrometry with a Digital Still Camera* (MS Thesis), University of Maryland, 2006.
[18] J.D. Maun, P.B. Sunderland, D.L. Urban, *Appl. Opt* 46 (2007) 483–488.
[19] R.B. Klimek, T.W. Wright, R.S. Sielken, *Color Image Processing and Object Tracking System*, NASA Lewis Research Center, 1996 Technical Memorandum No. 107144.
[20] J. Lei, N. Liu, *Combust. Flame* 167 (2016) 463–471.
[21] J. Lei, N. Liu, Y. Jiao, S. Zhang, *Proc. Combust. Inst* 36 (2016) 3149–3156.
[22] K.A. Hartl, A.J. Smits, *Combust. Flame* 163 (2016) 202–208.
[23] J. Lei, N. Liu, L. Zhang, K. Satoh, *Combust. Flame* 162 (2015) 745–758.
[24] R. Seiser, L. Truett, D. Trees, K. Seshadri, *Proc. Combust. Inst* 27 (1998) 649–657.

[25] M.J. Hargather, G.S. Settles, *Opt. Lasers Eng.* 50 (2012) 8–17.
[26] B. Fond, C. Abram, F. Beyrau, *Imaging Appl. Opt* (2014) (2014) LM1D.1.
[27] C. Abram, B. Fond, A.L. Heyes, F. Beyrau, *Appl. Phys. B Lasers Opt* 111 (2013) 155–160.
[28] J.H. Faler, *Some Experiments in Swirling Flows: Detailed Velocity Measurements of a Vortex Breakdown Using a Laser Doppler Anemometer* (Ph.D. Thesis), Cornell University, 1976.
[29] T. Sarpkaya, *J. Fluid Mech* 45 (1971) 545.
[30] J.H. Faler, S. Leibovich, *J. Fluid Mech* 86 (1978) 313–335.
[31] S.B. Hariharan, *The Structure of the Blue Whirl: A Soot-Free Reacting Vortex Phenomenon* (MS Thesis), University of Maryland, 2017.